Automatic Computer Aided Detection of Abnormalities in Multi-Parametric Prostate MRI

G.J.S. Litjens[a], P.C. Vos[a], J.O. Barentsz[a], N. Karssemeijer[a] and H.J. Huisman[a]

[a]Diagnostic Image Analysis Group, Radboud University Nijmegen Medical Centre
Geert Grooteplein Zuid 18, 6525 GA, Nijmegen, The Netherlands

ABSTRACT

Development of CAD systems for detection of prostate cancer has been a recent topic of research. A multi-stage computer aided detection scheme is proposed to help reduce perception and oversight errors in multi-parametric prostate cancer screening MRI. In addition, important features for development of computer aided detection systems for prostate cancer screening MRI are identified. A fast, robust prostate segmentation routine is used to segment the prostate, based on coupled appearance and anatomy models. Subsequently a voxel classification is performed using a support vector machine to compute an abnormality likelihood map of the prostate. This classification step is based on quantitative voxel features like the apparent diffusion coefficient (ADC) and pharmacokinetic parameters. Local maxima in the likelihood map are found using a local maxima detector, after which regions around the local maxima are segmented. Region features are computed to represent statistical properties of the voxel features within the regions. Region classification is performed using these features, which results in a likelihood of abnormality per region. Performance was validated using a 188 patient dataset in a leave-one-patient-out manner. Ground truth was annotated by two expert radiologists. The results were evaluated using FROC analysis. The FROC curves show that inclusion of ADC and pharmacokinetic parameter features increases the performance of an automatic detection system. In addition it shows the potential of such an automated system in aiding radiologists diagnosing prostate MR, obtaining a sensitivity of respectively 74.7% and 83.4% at 7 and 9 false positives per patient.

Keywords: prostate cancer, MRI, CAD, detection

1. INTRODUCTION

Prostate cancer is a large health problem in modern Western society, being the second largest cause of death in male cancers.[1] In the last decade, prostate cancer screening has been receiving increasing attention. Recently, a large prostate specific antigen (PSA) prostate cancer screening study (with systematic transrectal ultrasound (TRUS) guided biopsies) was completed.[2] A reduction in mortality of up to 20% could be achieved,[2] however, to save one life, 1410 men had to be screened and 48 cancers had to be treated, which is considered severe overtreatment, as most of these men will not die due to prostate cancer. Thus it is important to find a way to improve the specificity of prostate cancer screening.

Magnetic resonance imaging (MRI) has become a useful tool in the diagnosis of prostate cancer, achieving higher sensitivity (up to 81%) and specificity (up to 96%) while being a non-invasive technique.[3,4] Using MRI as a second line screening modality can help reduce the number of unnecessary biopsies and allow localization and targeted biopsies, which in turn leads to a better assessment of cancer aggressiveness.[5] A typical prostate MRI dataset consists of several image volumes, for example an apparent diffusion coefficient (ADC) map, a dynamic contrast enhanced (DCE) time series and T2-weighted images. In addition, pharmacokinetic parameter maps can be calculated from the DCE series using pharmacokinetic modeling.

Screening with MRI would require the radiologists to read enormous amounts of images, while prostate MRI requires specific expertise which is not widely available. Computer aided detection of prostate cancer could simplify the task of the radiologist by indicating suspicious regions and reducing oversight and perception errors.

Prostate cancer CAD systems are a recent and growing research topic. Langer et al.[6] used a logistic regression analysis in multi-parametric MRI for the detection of prostate cancer. In addition, Puech et al.[7]

Medical Imaging 2011: Computer-Aided Diagnosis, edited by Ronald M. Summers, Bram van Ginneken,
Proc. of SPIE Vol. 7963, 79630T · © 2011 SPIE · CCC code: 0277-786X/11/$18 · doi: 10.1117/12.877844

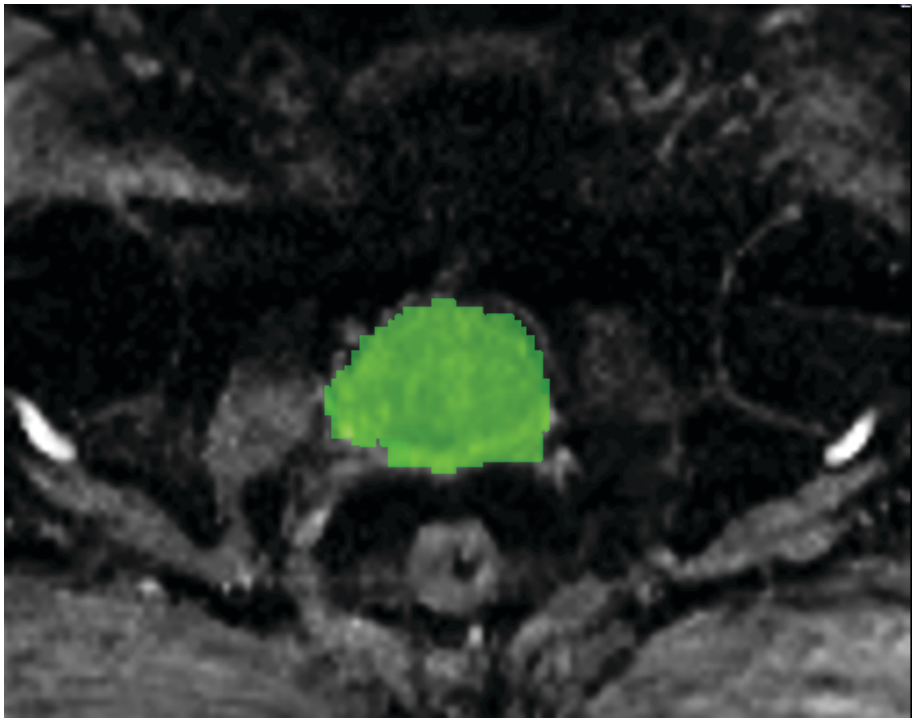

Figure 1. Example of a prostate segmentation. Results are projected on the ADC map of the patient

developed a CAD system using seeded region growing of suspicious regions in combination with DCE-MRI data to do computer aided diagnosis of prostate cancer. In this study we investigate a fully automatic prostate cancer detection system for multi-parametric MRI, using a two stage classification strategy. This system is also used to assess the added value of commonly used features in prostate cancer MRI in a computer aided detection scheme.

2. METHODS

A two-stage classification scheme was used to estimate the likelihood of abnormality of prostate regions. We applied a fast and robust segmentation algorithm to segment the prostate, after which a 3D likelihood map was generated using a support vector machine classifier (SVM) trained with quantitative voxel features. Points of interest were found using a local maxima detector on the likelihood map, after which a region was segmented around each local maximum. For every region statistics of the voxel features were calculated. A second classifier then computed region based likelihoods.

2.1 Prostate Segmentation

It is key to have a fast, fully automatic and robust segmentation of the prostate. A recently developed technique in our group was used for this purpose. The segmentation uses a novel paradigm based on coupled parametric anatomy and appearance models. These models are mutually dependent through a probabilistic population model, restricting position and size of the prostate based on the size and position of other organs. The fact that certain positions are correlated i.e. the bladder is always in front of the prostate, allows us to reduce the number of independent parameters. The population mean and standard deviations of the parameters were obtained from independent patient datasets. The appearance model was based on the ADC map. The pelvic anatomy and appearance models were fitted to the image using a quasi-Newton optimization. The cost function was defined as a sum of the deviations from the population model in the appearance and anatomical models and a similarity term. Because the entire optimization routine is based on relatively few parameters it is quite fast and robust. An example result is shown in figure 1

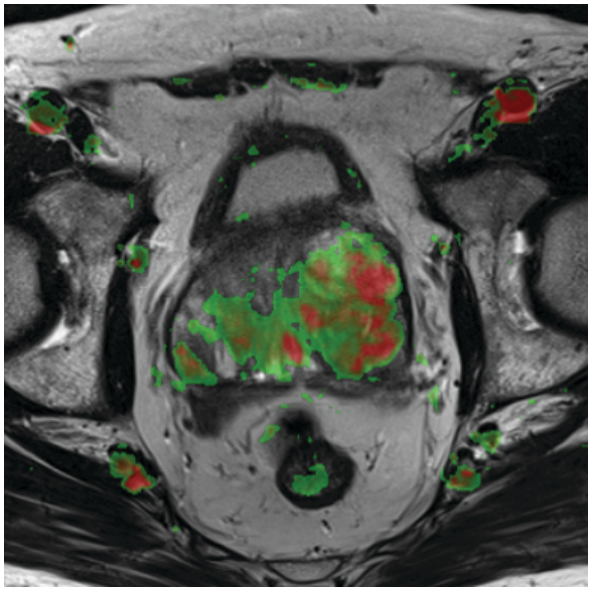

(a) T2-weighted image with K^{trans} parameter map overlayed. Red indicates high values, green indicates low values and transparent regions indicate values close to zero

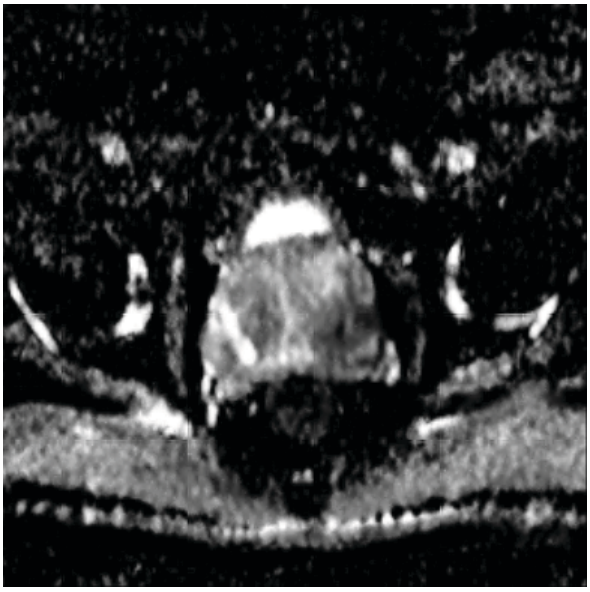

(b) ADC map of the prostate, high intensity regions indicate high ADC values

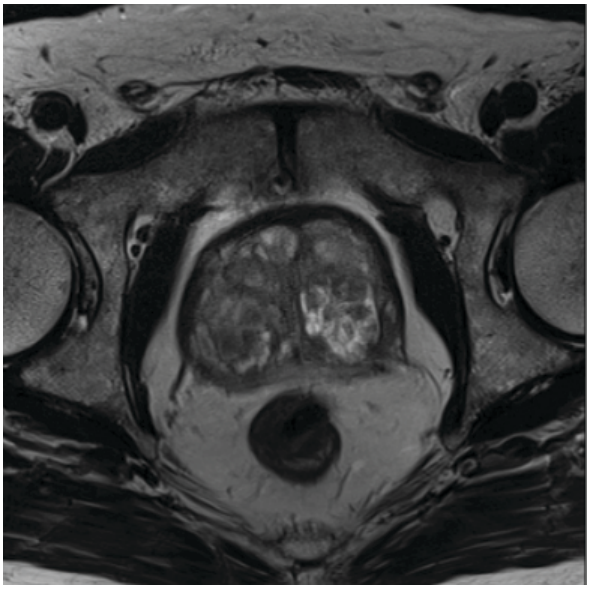

(c) T2-weighted image of the prostate

Figure 2. Examples of prostate MR images from which features are extracted for classifier training. The prostate is in the center of each image.

2.2 Voxel Feature Extraction

It has been shown that pharmacokinetic features, obtained from the DCE series have diagnostic potential.[8] In this paper we used two pharmacokinetic features, K^{trans} and k_{ep}. The calculation of these parameters is performed using an automatic reference tissue approach to estimate the arterial input function.[9] The ADC has also been shown to have diagnostic value.[4,10] In addition, T2-weighted images have traditionally been used to diagnose prostate cancer.[4] An example of such a set of images is shown in figure 2.

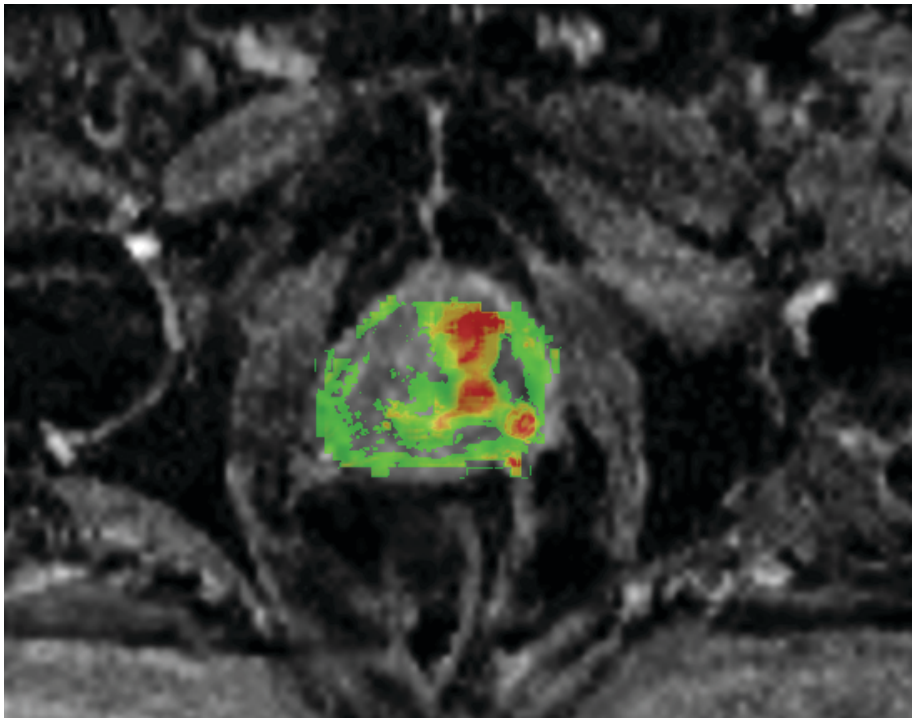

Figure 3. Example of a prostate cancer likelihood map, where darker regions (red) represent areas of high likelihood. Results are projected on the ADC map of the patient

Prostate cancer usually has the appearance of a blob, either dark or bright depending on the MR acquisition, i.e. dark on ADC, bright on K^{trans}. Thus on all feature maps a multi-scale Hessian blob detector was used to give a blobness measure for that feature. Three scales were used ranging from 8 mm to 12 mm in diameter and the blob detector was normalized for each scale. The maximum blobness output at each spatial location was computed. The features maps were resampled such that they all have the same dimensions. Additionally, 4 position features were calculated using the x, y and z distances of each voxel to the prostate center, which was obtained from the prostate segmentation. The fourth position feature was the Euclidean distance to the prostate center. These positions were used because the prostate consists of three distinct zones. This way we have an indication in which zone a feature vector was obtained.

2.3 Voxel Classification

The voxel classifier computes a likelihood for each voxel of being abnormal using an SVM classifier with a Radial Basis Kernel.[11] The SVM is trained with parameter optimization (C and γ) using 5-fold cross-validation and grid search. In addition feature values were normalized by subtracting the mean and subsequent division with the standard deviation. An example of a likelihood map obtained from the voxel classification is shown in figure 3

2.4 Region Feature Extraction

A local maxima detector is used with a kernel of 12 mm in diameter, if the middle voxel in the kernel is the maximum inside the kernel it is noted as a local maximum. Convoluting this kernel with the likelihood map results in a number of local maxima. All maxima with a voxel likelihood higher than 50% are selected for further analysis. A spherical region is segmented around the peak maximum (10 mm diameter) from which the feature statistics are calculated (mean, standard deviation, 50, 75 and 90-percentiles), we are also currently working a lesion segmentation algorithm to allow a more accurate segmentation.

2.5 Region classification

A region classifier is trained in a similar fashion as the voxel classifier, using SVM, cross-validation and grid search for parameter optimization and feature value normalization. This classifier computes a likelihood for each region of being abnormal.

3. VALIDATION

In 2009, 188 men with high PSA levels which had at least one previous negative biopsy guided by TRUS underwent an MRI scan. Two expert radiologists annotated suspicious findings requiring biopsy in 150 men. All were scanned with the same protocol on a Siemens 3T MRI scanner, which gave an ADC map (calculated by the scanner software), a DCE time series and T2-weighted images. The radiologists annotated the findings using an image analysis package. The findings were then manually segmented by two experts using a voxel painting tool.

Training data for the voxel classifier was selected from the ground truth annotations and random locations within the prostate segmentations in a balanced manner. Normal voxel features vectors were only obtained from healthy men. For the region classifier feature vectors were obtained from the manually segmented ground truth and from regions obtained in healthy patients through the local maxima detection and region segmentation.

After collecting the training data our approach was validated on the same patient data set, in a leave-one-patient-out manner. When a patient was classified the training data corresponding to this patient was removed and the classifiers retrained before classification. A local maximum is defined as a hit when its region overlaps with the manual segmentation of the ground truth, otherwise it is a false positive in the first classification stage. This step determines the total sensitivity of the system.

In the second stage classification we use FROC analysis to determine the performance of our system based on the likelihoods obtained for each region and the ground truth. A region is considered a hit when it overlaps with the manual segmentation of the ground truth. Each manual segmentation can only obtain one hit, when multiple regions overlap the manually segmented ground truth the region with the biggest overlap is chosen, the rest is discarded.

Four different feature sets where used to assess the importance of certain features in the detection of prostate cancer. One set consists of only T2-weighted image features, there is a set for both pharmacokinetic features and ADC features in combination with T2-weighted image features and one set consists of all features.

4. RESULTS

Our initial detector step has a sensitivity of 94.7%, which means we miss 5.3% of the abnormal regions. The FROC curves are corrected for this, thus maximum performance in the second stage classification is 94.7%. FROC curves were constructed for several feature sets. In clinical research it has been shown that the ADC and DCE MRI increase the sensitivity and specificity of diagnosis by radiologists.[4] This can also be seen in figure 4, were the sensitivity at every number of false positives is higher when including either ADC or pharmacokinetic features when compared to just using T2-weighted features.

The total performance of our fully automatic CAD system is 74.7% and 83.4% sensitivity at 7 and 9 false positives per patient respectively when using all features, which is a reasonable result for a first iteration of such a system.

5. DISCUSSION

A multi-modal, fully automatic MRI prostate cancer detection scheme using CAD has been proposed, which has potential in assisting radiologists in detecting prostate cancer in MRI. The FROC curves further demonstrate that the inclusion of both diffusion and dynamic contrast enhanced features can lead to improvements in the CAD system, which reproduces results from literature on clinical research.

It is remarkable that our pharmacokinetic features perform so well, it has been shown previously that they do not add much information,[4] however, often an assumed arterial input function is used. In our scheme a reference tissue approach is used, which might lead to more accurately calculated pharmacokinetic features.

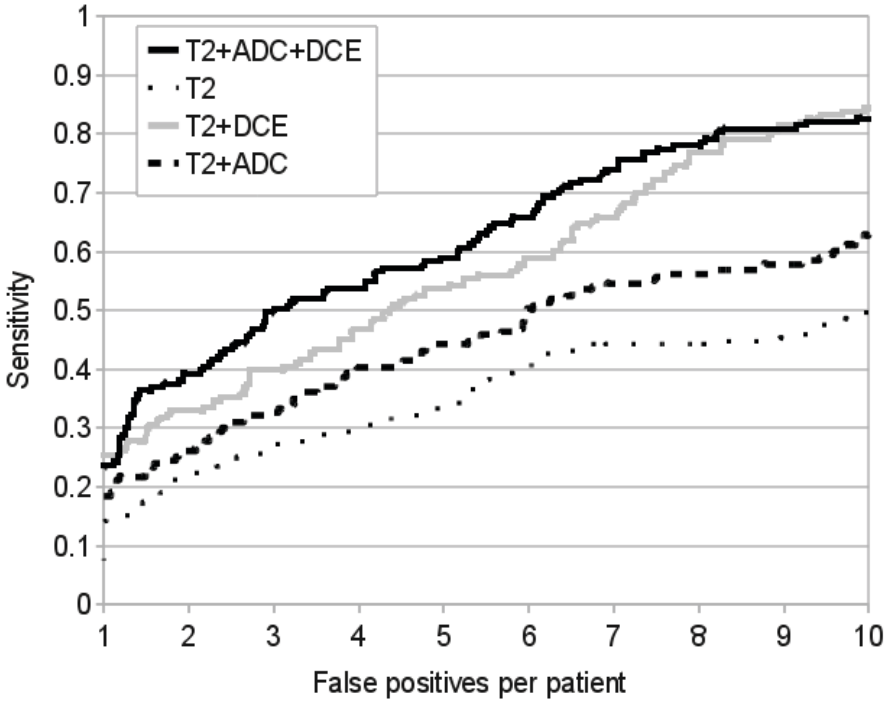

Figure 4. FROC curves for the fully automatic CAD system. Different FROC curves represent different inclusion of features sets

A number of improvements can still be made. For example, patient population consists of men who have had a previous biopsy. As we would like to use the prostate cancer detection system in a screening setting this population is biased. This population is in fact more difficult to analyze, as we know that the 'easy' cases are already filtered out by the transrectal ultrasound biopsy.

The prostate segmentation could be refined to use multiple MRI acquisitions in its appearance model, for example T2-weighted images. Additionally, a subdivision segmenting peripheral, transition and central zone separately could be made, which would allow a better classification of the regions within each zone, compared to using the positions relative to the center of the segmentation mask.

Obtaining the region features around the peak likelihoods could be done more thoroughly using a lesion segmentation instead of a predefined region. Then we could also incorporate morphological features. Additionally, radiologists also look at symmetry in for example pharmacokinetic maps in the prostate. Developing symmetry features might thus also improve the performance of our system.

Summarizing, we present a novel prostate cancer detection system using a two-stage classification strategy based on a voxel and region classification in series, which gives promising results in a 188 patient dataset. In addition, we have shown that inclusion of ADC and pharmacokinetic features can improve detection performance.

REFERENCES

[1] Wolf, A. M. D., Wender, R. C., Etzioni, R. B., Thompson, I. M., D'Amico, A. V., Volk, R. J., Brooks, D. D., Dash, C., Guessous, I., Andrews, K., DeSantis, C., Smith, R. A., and Committee, A. C. S. P. C. A., "American cancer society guideline for the early detection of prostate cancer: update 2010.," *CA Cancer J Clin* **60**(2), 70–98 (2010).

[2] Schröder, F. H., Hugosson, J., Roobol, M. J., Tammela, T. L. J., Ciatto, S., Nelen, V., Kwiatkowski, M., Lujan, M., Lilja, H., Zappa, M., Denis, L. J., Recker, F., Berenguer, A., Mttnen, L., Bangma, C. H., Aus, G., Villers, A., Rebillard, X., van der Kwast, T., Blijenberg, B. G., Moss, S. M., de Koning, H. J., Auvinen,

A., and Investigators, E. R. S. P. C., "Screening and prostate-cancer mortality in a randomized european study.," *N Engl J Med* **360**, 1320–1328 (Mar 2009).

[3] Turkbey, B., Pinto, P. A., Mani, H., Bernardo, M., Pang, Y., McKinney, Y. L., Khurana, K., Ravizzini, G. C., Albert, P. S., Merino, M. J., and Choyke, P. L., "Prostate cancer: value of multiparametric mr imaging at 3 t for detection–histopathologic correlation.," *Radiology* **255**, 89–99 (Apr 2010).

[4] Kitajima, K., Kaji, Y., Fukabori, Y., ichiro Yoshida, K., Suganuma, N., and Sugimura, K., "Prostate cancer detection with 3 T MRI: comparison of diffusion-weighted imaging and dynamic contrast-enhanced MRI in combination with T2-weighted imaging.," *J Magn Reson Imaging* **31**, 625–631 (Mar 2010).

[5] Langer, D. L., van der Kwast, T. H., Evans, A. J., Plotkin, A., Trachtenberg, J., Wilson, B. C., and Haider, M. A., "Prostate tissue composition and mr measurements: investigating the relationships between adc, t2, k(trans), v(e), and corresponding histologic features.," *Radiology* **255**, 485–494 (May 2010).

[6] de Lange, E. E., Altes, T. A., Patrie, J. T., Battiston, J. J., Juersivich, A. P., Mugler, J. P., and Platts-Mills, T. A., "Changes in regional airflow obstruction over time in the lungs of patients with asthma: evaluation with 3he mr imaging.," *Radiology* **250**, 567–575 (Feb 2009).

[7] Puech, P., Potiron, E., Lemaitre, L., Leroy, X., Haber, G.-P., Crouzet, S., Kamoi, K., and Villers, A., "Dynamic contrast-enhanced-magnetic resonance imaging evaluation of intraprostatic prostate cancer: correlation with radical prostatectomy specimens.," *Urology* **74**, 1094–1099 (Nov 2009).

[8] Vos, P. C., Hambrock, T., Barentsz, J. O., and Huisman, H. J., "Computer-assisted analysis of peripheral zone prostate lesions using T2-weighted and dynamic contrast enhanced T1-weighted MRI," *Physics in Medicine and Biology* **55**(6), 1719–1734 (2010).

[9] Vos, P. C., Hambrock, T., Barentsz, J. O., and Huisman, H. J., "Automated calibration for computerized analysis of prostate lesions using pharmacokinetic magnetic resonance images.," in [*Medical Image Computing and Computer-Assisted Intervention*], *Lecture Notes in Computer Science* **12**, 836–843 (2009).

[10] Rosenkrantz, A. B., Kopec, M., Kong, X., Melamed, J., Dakwar, G., Babb, J. S., and Taouli, B., "Prostate cancer vs. post-biopsy hemorrhage: diagnosis with t2- and diffusion-weighted imaging.," *J Magn Reson Imaging* **31**, 1387–1394 (Jun 2010).

[11] Chang, C.-C. and Lin, C.-J., *LIBSVM: a library for support vector machines* (2001). Software available at `http://www.csie.ntu.edu.tw/~cjlin/libsvm`.